



# Differences in action potential and early afterdepolarization properties in LQT2 and LQT3 models of long QT syndrome

\*<sup>1</sup>Christian R. Studenik, <sup>2</sup>Zhengfeng Zhou & <sup>2</sup>Craig T. January

<sup>1</sup>Institute of Pharmacology and Toxicology, University of Vienna, Vienna, Austria and <sup>2</sup>Section of Cardiology, University of Wisconsin, Madison, Wisconsin, U.S.A.

**1** Long QT syndrome has many causes from both acquired and congenital disorders. For the congenital disorders, their presentation and disease course are not identical. We studied two pharmacological models of long QT syndrome (LQT) to identify differences in cellular electrophysiological properties that may account for this. LQT2 was simulated by suppression of the rapidly activating delayed rectifier potassium current ( $I_{Kr}$ ) with the drug E-4031, and LQT3 was simulated by slowing of the sodium current ( $I_{Na}$ ) decay with the toxin ATX II.

**2** Single rabbit ventricular cell action potentials were studied using the amphotericin B perforated patch clamp technique. Action potential and early afterdepolarization (EAD) properties were rigorously defined by the frequency power spectra obtained with fast Fourier transforms.

**3** The E-4031 ( $n=43$  myocytes) and ATX II ( $n=50$  myocytes) models produced different effects on action potential and EAD properties. The major differences are that ATX II, compared with E-4031, caused greater action potential prolongation, more positive plateau voltages, lower amplitude EADs with less negative take-off potentials, greater time to the EAD peak voltage, and longer duration EADs. Despite causing greater action potential prolongation, the incidence of EAD induction was much less with the ATX II model (28%) than with the E-4031 model (84%). Thus these two pharmacological models have strikingly different cellular electrophysiological properties.

**4** Our findings provide cellular mechanisms that may account for some differences in the clinical presentation of LQT2 and LQT3.

*British Journal of Pharmacology* (2001) **132**, 85–92

**Keywords:** Long QT syndrome; early afterdepolarizations; E-4031; ATX II; fast Fourier transforms; rabbit ventricular myocytes

**Abbreviations:** EAD, early afterdepolarization; FFT, fast Fourier transform; HERG, human-ether-a-go-go-related gene;  $I_{Kr}$ , rapidly activating delayed rectifier potassium current;  $I_{Na}$ , sodium current; LQT, long QT syndrome

## Introduction

In the congenital and acquired forms of the long QT syndrome (LQT) two ion channel targets for modification are the rapidly activating delayed rectifier  $K^+$  channel current ( $I_{Kr}$ ) and the  $Na^+$  channel current ( $I_{Na}$ ). Drug suppression of  $I_{Kr}$ , which has been used to model chromosome 7-linked congenital LQT (LQT2), is known to cause action potential prolongation and the induction of early afterdepolarizations (EADs) arising from plateau voltages, along with QT interval prolongation and the arrhythmia torsades de pointes (Roden, 1993; Colatsky & Argentieri, 1994; Zhou *et al.*, 1995; Vorperian *et al.*, 1996; January & Zhou, 1997; Shimizu & Antzelevitch, 2000). Similarly, modification of  $I_{Na}$  with sea anemone toxins such as ATX II, which has been used to model chromosome 3-linked congenital LQT (LQT3), slows the rate of channel inactivation to produce action potential prolongation and plateau EADs, QT interval prolongation and torsades de pointes (El-Sherif *et al.*, 1988; Boutjdir & El-Sherif, 1991; Shimizu & Antzelevitch, 2000). In congenital LQT, mutations of these ion channels have

been associated with phenotypically distinct electrocardiographic patterns (Moss *et al.*, 1995) and with different clinical prognoses (Zareba *et al.*, 1998). These findings suggest that the cellular electrophysiological properties associated with different ion channel gene defects or channel interventions may differ.

In the present work, we studied two pharmacological models of LQT in isolated rabbit ventricular myocytes to identify differences in underlying cellular electrophysiological properties. The isolated rabbit heart is an established model for studying mechanisms of torsades de pointes (D'Alonzo *et al.*, 1997; Zabel *et al.*, 1997; Eckhardt *et al.*, 1999). In rabbit ventricular myocytes the delayed rectifier  $K^+$  channel current is thought to represent mostly  $I_{Kr}$  (Carmeliet, 1992; Clay *et al.*, 1995; Zhou *et al.*, 1995). We used the class III methanesulphonamide antiarrhythmic drug E-4031 to block  $I_{Kr}$  and simulate LQT2, and the sea anemone toxin ATX II to delay  $Na^+$  channel inactivation and simulate LQT3. We studied action potential and EAD properties using the perforated patch clamp technique to avoid intracellular dialysis and ion channel current rundown that occurs with the conventional ruptured patch technique. We also employed fast Fourier transforms (FFTs) to rigorously define the EAD frequency power spectra and to separate

\*Author for correspondence at: Institute of Pharmacology and Toxicology, Althanstrasse 14, A-1090 Vienna, Austria.  
E-mail: Christian.Studenik@univie.ac.at

EADs from irregular low amplitude membrane voltage oscillations found in the ATX II model. Our data show that these two LQT models produce strikingly different effects on action potential and EAD electrophysiological properties.

Preliminary reports of this work have appeared (Studenik *et al.*, 1996; 1999).

## Methods

### *Single rabbit ventricular cell isolation procedure*

Rabbit ventricular cells were isolated by enzymatic dispersion (Verperian *et al.*, 1996). Briefly, the rabbits were anaesthetized with Ketamine HCl (80–100 mg kg<sup>-1</sup>), Xylazine HCl (3–5 mg kg<sup>-1</sup>) and sodium pentobarbital (50 mg kg<sup>-1</sup>). Hearts were excised and perfused with normal Tyrode's solution for 4 min, nominally Ca<sup>2+</sup>-free Tyrode's solution for 5 min, and Tyrode's solution containing albumin (1 mg ml<sup>-1</sup>), protease (0.1 mg ml<sup>-1</sup>) and collagenase (0.6 mg ml<sup>-1</sup>) for 8 min. After enzyme perfusion the right and left ventricles were cut into small pieces and incubated in fresh enzyme solution containing collagenase (1 mg ml<sup>-1</sup>) and protease (0.1 mg ml<sup>-1</sup>) for 10 min at 37°C while being agitated in a shaking water bath. Regional differences in cellular electrophysiological properties were not studied. The isolated myocytes were stored in a solution containing (mM): K-glutamate 130, MgCl<sub>2</sub> 5.7, EGTA 0.1, and HEPES 10.

### *Perforated patch-clamp recording technique*

Membrane voltage was recorded in whole cell current clamp configuration using the amphotericin B perforated patch method (Rae & Cooper, 1990; Zhou *et al.*, 1995; Vorperian *et al.*, 1996; Zhou & January, 1998). Amphotericin forms monovalent selective (cations>anions) channels in the cell membrane that provide electrical access to the cell interior. Amphotericin B (60 mg ml<sup>-1</sup>) was dissolved in DMSO and then added to internal pipette solution at final concentration of 240 µg ml<sup>-1</sup>. The internal pipette solution contained (in mM): K-glutamate 100, KCl 40, NaCl 0 or 5, EGTA 1, HEPES 10 (pH titrated to 7.2 with KOH). With the amphotericin B method, the access resistances usually were 4–10 MΩ. The external solution contained (in mM): NaCl 137, KCl 4.0, CaCl<sub>2</sub> 1.8, MgCl<sub>2</sub> 1.0, glucose 10, HEPES 10 (pH titrated to 7.4 with NaOH). A Dagan 3900 patch clamp amplifier was used to record action potentials which were elicited by applying 1 ms long depolarizing current pulses through the patch electrode at 0.5 Hz. All experiments were performed at 36 ± 1°C.

### *Data analysis*

Computer software (pCLAMP, version 6.02, Axon Instruments) was used to generate recording protocols. Data were digitized at 1 kHz and were stored for later analysis. Fast Fourier transforms (Bergland, 1969) were performed to analyse the repolarization phase of the action potential. The FFT method converts the time-domain into the frequency-domain and plots signal power (I<sup>2</sup>) versus frequency content (Hz).

### *Drugs and toxins*

E-4031 was obtained from Eisai Ltd (Ibaraki, Japan) and was dissolved in distilled water to give a stock solution of 1 mM. ATX II was obtained from Sigma Chemicals (St. Louis, MO, U.S.A.) and was dissolved in distilled water to give a stock solution of 100 µM. In preliminary experiments, we identified the maximal drug and toxin concentrations that caused action potential prolongation but did not cause failure of the myocytes to repolarize to the resting potential. These drug concentrations (20 nM for E-4031 and 30 nM for ATX-II) were used in all subsequent experiments (*n* = 43 myocytes for E-4031, *n* = 50 myocytes for ATX II). Drug concentrations exceeding these (≥ 30 nM E-4031 and 40 nM ATX II) frequently caused failure of rapid repolarization with the membrane voltage remaining at the plateau range. Ryanodine, thapsigargin and tetrodotoxin (TTX) were obtained from Sigma Chemicals (St. Louis, MO, U.S.A.).

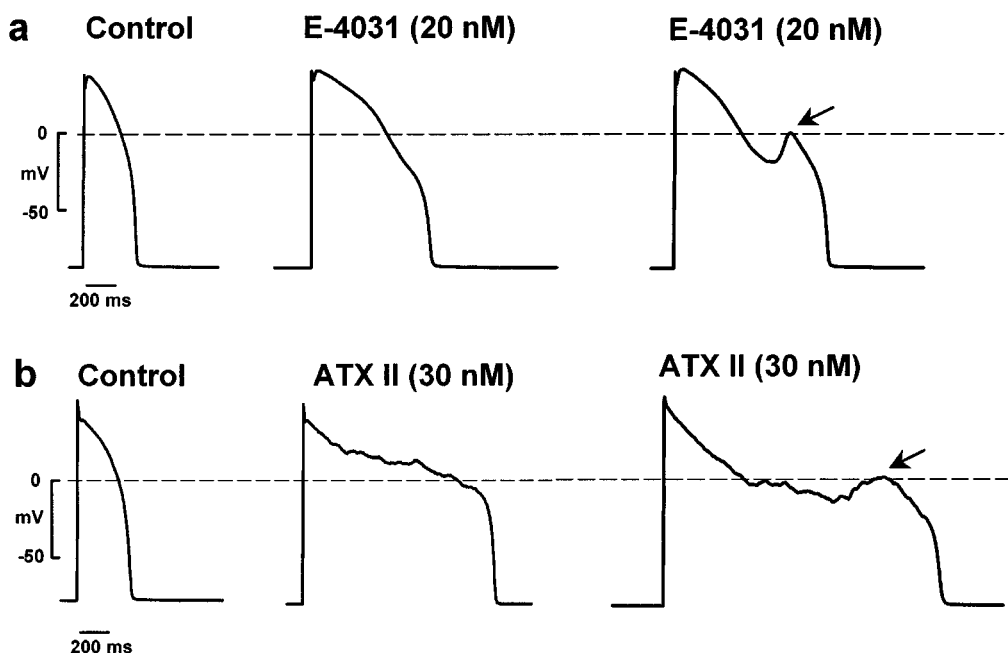
### *Statistical methods*

Where appropriate, data are given as the mean ± standard deviation. Statistical significance was tested using a paired or Student's *t*-test.

## Results

The effect of E-4031 on rabbit ventricular cell action potentials is shown in the Figure 1a. Initially it caused the control action potential (left trace) to prolong (middle trace) which was followed by the development of an EAD (right trace, arrow, take-off potential of -19 mV) that preceded repolarization. EADs in the E-4031 model were easily distinguished as secondary depolarizations at action potential plateau voltages. In this myocyte the control resting potential was -84 mV and action potential amplitude was 130 mV which did not change after drug exposure. The effect of ATX II on rabbit ventricular cell action potentials in a different myocyte is shown in Figure 1b. ATX II initially caused the control action potential (left trace) to markedly prolong with the simultaneous appearance of irregular low amplitude membrane voltage oscillations (middle trace, see also El-Sherif *et al.*, 1990). ATX II consistently induced these irregular low amplitude membrane voltage oscillations during the plateau in all myocytes studied (*n* = 50), whereas this type of activity was never observed in myocytes exposed to E-4031 (*n* = 43). In some myocytes, ATX II exposure was followed by the development of a small amplitude EAD (right trace, arrow, take-off potential of -9 mV) which preceded repolarization. In this myocyte the control resting potential was -83 mV and action potential amplitude was 128 mV which did not change with toxin exposure.

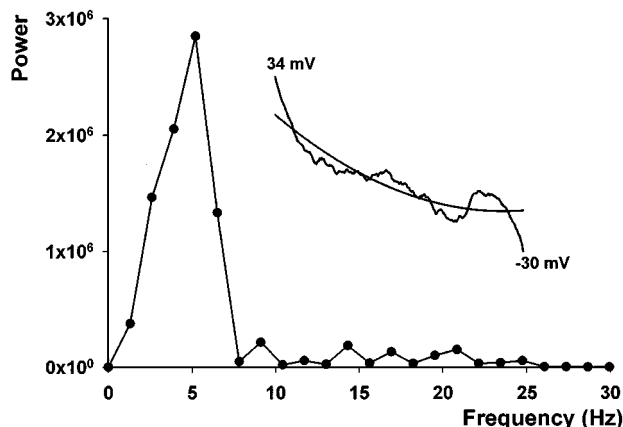
With the ATX II model, the irregular low amplitude membrane voltage oscillations could be difficult to distinguish from EADs. To develop quantitative criteria for the presence of EADs, we used FFTs to analyse the frequency power spectra of all myocytes exposed to E-4031 and ATX II. For calculation of the FFT, each recorded action potential data set was truncated from the peak voltage of the action potential normally to -30 mV of repolarization. This region contains the action potential plateau and EADs, and in the



**Figure 1** Effects of E-4031 and ATX II on rabbit ventricular action potentials recorded using the perforated patch method. (a) Shows the effect of E-4031 and (b) shows the effect of ATX II. Arrows indicate EADs.

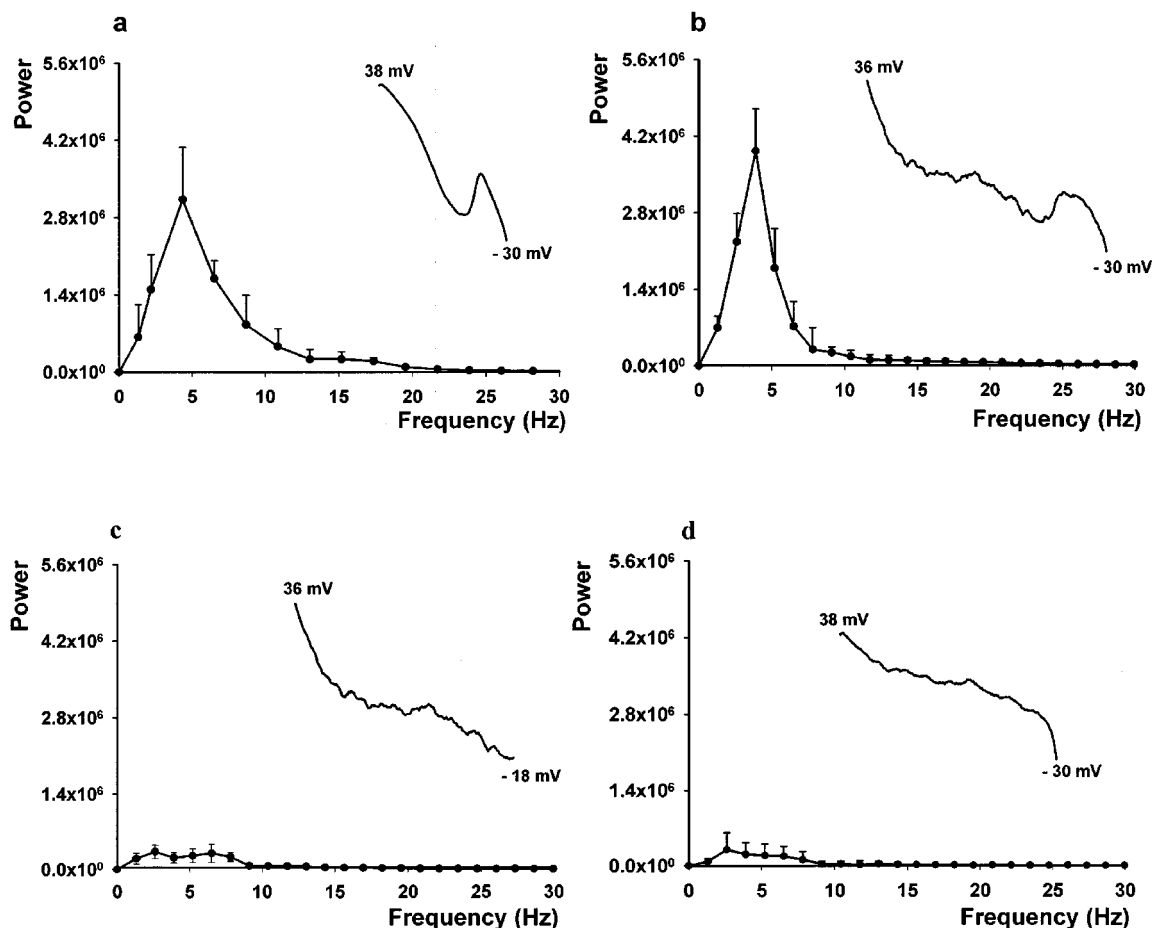
ATX II model it also contained the irregular low amplitude membrane voltage oscillations. The resting potential, action potential upstroke and rapid repolarization phase negative to  $-30$  mV were excluded from analysis since the EADs we studied do not arise during these portions of the action potential, and contamination of FFTs by the frequency content of these signals was avoided. To perform the FFT, each data set was fit with a nonlinear regression line. These were subtracted to give a difference signal to minimize frequency interference, and the frequency content was analysed. Figure 2 shows an individual FFT power spectrum record obtained following ATX II exposure in a myocyte, with the truncated action potential record and nonlinear regression fit to it shown in the inset. The FFT contained a discrete power peak at around 5 Hz.

Figure 3 shows averaged FFTs for the E-4031 and ATX II treated myocytes. Of 43 myocytes exposed to E-4031, 36 (84%) developed EADs (see example truncated action potential record in the inset in Figure 3a). The averaged FFT for these myocytes shows a discrete peak in the frequency power spectrum at about 5 Hz. In every E-4031 treated myocyte that developed EADs, the power spectrum peak amplitude exceeded  $2.2 \times 10^6$  units. In the myocytes ( $n=7$ ) not generating EADs, there was no discrete peak in the FFT and the power spectrum maximum amplitude was less than  $0.5 \times 10^6$  units (data not shown). For ATX II treated myocytes, EAD activity (see truncated action potential record in the inset in Figure 3b) was observed in 14 of 50 myocytes (28%). The individual FFTs for each myocyte with EADs showed a discrete peak in the frequency power spectrum between 4–5 Hz and the peak power amplitude exceeded  $2.8 \times 10^6$  units. The averaged FFT for these myocytes is shown in Figure 3b and it contains a discrete peak in the frequency power spectrum at about 5 Hz, similar to that found in myocytes with E-4031 induced



**Figure 2** Fast Fourier transform analysis of the frequency power spectrum of an action potential plateau in an ATX II treated myocyte. The FFT shows a discrete power peak at about 5 Hz along with low amplitude signals at higher frequencies. The inset shows the original truncated action potential recording from its peak voltage of 34 to  $-30$  mV and the nonlinear regression fit. The truncated action potential record contains irregular low amplitude membrane voltage oscillations and an EAD.

EADs. The data from these 14 myocytes were then re-analysed after truncating the repolarization record of each action potential to before the onset of the EAD (see truncated action potential record in the inset in Figure 3c, same record as used in inset in Figure 3b), thus eliminating the EAD from the reanalysis. The resulting averaged FFT is plotted in Figure 3c, and shows a frequency power spectrum with no discrete power peak and a low power amplitude. Finally, we analysed the remaining 36 myocytes treated with ATX II that developed irregular low amplitude membrane voltage oscillations but no EAD activity. The averaged FFT



**Figure 3** Averaged frequency power spectra of myocytes exposed to E-4031 and ATX II. (a) Shows the FFTs of 36 myocytes exposed to E-4031 that developed EADs. (b) Shows the FFTs from 14 myocytes exposed to ATX II that developed EADs. (c) Shows the FFTs of the same 14 myocytes after truncating the repolarization record of each action potential before the onset of EADs. (d) Shows the FFTs of 36 myocytes treated with ATX II that developed irregular low amplitude membrane voltage oscillations but without EAD activity. The inset in each panel shows a representative action potential record truncated from the peak action potential voltage to  $-30$  mV (a,b,d) or to the EAD take-off potential (c).

is plotted in Figure 3d with the inset showing an example truncated action potential record. The FFT shows a low amplitude frequency power spectrum and it lacked a discrete peak at about 5 Hz, similar to that shown in Figure 3c. We conclude from these data that the presence of a discrete peak in the FFT power spectrum between 4–5 Hz with a peak amplitude exceeding  $2.2 \times 10^6$  units represents power added from EADs occurring during the terminal portion of the action potential plateau. Particularly for the ATX II model, it provides a quantitative approach for identifying and separating EADs from ATX II induced irregular low amplitude membrane voltage oscillations which lack these properties.

Using the FFT approach to confirm the presence of EADs, we then analysed properties of the initial action potential that contained an EAD following exposure to E-4031 or ATX II. These data are summarized in Table 1. The data show that the resting potential and action potential amplitudes were similar for control conditions and after the development of EADs in both the E-4031 ( $n=36$  myocytes) and ATX II ( $n=14$  myocytes) groups. However, for E-4031 treated cells compared to ATX II treated cells, the EAD take-off potential was more negative, EAD amplitude was larger, EAD peak

voltage was reached earlier, and the EAD duration was less. The action potential plateau voltages also differed between the two models as previously shown in Figure 1. Figure 4a shows averaged data for control action potentials and the last action potential *before* the development of an EAD in the same groups of myocytes (E-4031,  $n=36$ , and ATX II,  $n=14$ ). Action potential plateau voltages were measured at 100 ms increments following the action potential upstroke. For the two groups of myocytes, the control action potential voltages at 100, 200 and 300 ms following the upstroke were similar ( $P>0.05$  at each time point), and action potentials had repolarized by 400 ms. Following exposure to E-4031 or ATX II, the action potentials prolonged prior to developing EADs, however, the plateau voltages and durations preceding the onset of repolarization were different as shown in Figure 4b. For an example, following E-4031 exposure the plateau voltage was  $-18.9 \pm 4.1$  mV at an action potential duration of 600 ms ( $n=36$  myocytes). Following this, the action potentials began to rapidly repolarize. For ATX II the action potential plateau voltage was more positive and the action potential durations were longer. For example, the plateau voltage at an action potential duration of 600 ms ( $n=14$  myocytes) was  $7.8 \pm 3.2$  mV, and it reached  $-10.1 \pm 3.7$  mV

**Table 1** Resting and action potential amplitudes and EAD parameters in control and after addition of E-4031 and ATX II

	Control (n=36)	E-4031 (n=36)	Control (n=14)	ATX II (n=14)
RP (mV)	-83.4±3.8	-83.6±1.7	-82.3±1.9	-81.4±1.2
AP amp (mv)	131.3±4.3	129.2±5.2	130.4±3.6	129.8±3.5
TOP (mV)	-	-18.9±4.1	-	-10.1±3.7*
EAD amp (mV)	-	27.1±5.2	-	16.4±3.1**
Time to EAD (ms)	-	675.0±67.5	-	1470.0±95.7***
EAD duration (ms)	-	201.7±19.8	-	267.3±20.7**

RP=resting potential, AP amp=action potential amplitude, TOP=EAD take-off potential, EAD amp=EAD amplitude (calculated as the difference between TOP and EAD peak voltage), Time to EAD=time from action potential upstroke to EAD peak voltage, EAD duration=duration of the EAD (calculated as the time required for the membrane voltage during an EAD to return to the TOP). \* $P<0.05$ , \*\* $P<0.01$  or \*\*\* $P<0.001$  between drug groups.

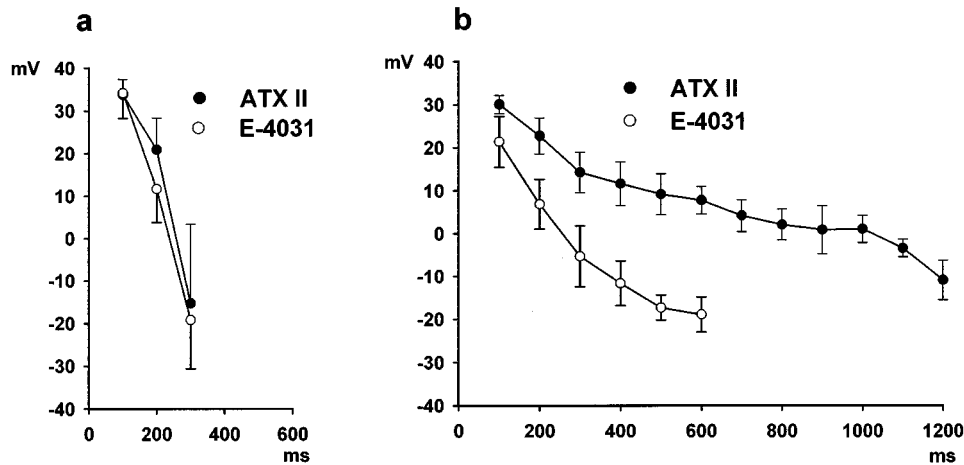


**Figure 4** Averaged action potential plateau voltages measured at 100 ms increments following the action potential upstroke. (a) Shows data for the control action potentials recorded before exposure to E-4031 ( $n=36$  myocytes) or ATX II ( $n=14$  myocytes). For control conditions repolarization was complete by 400 ms. (b) Shows data for the same myocytes for action potentials prolonged by exposure to E-4031 ( $n=36$  myocytes) and ATX II ( $n=14$  myocytes) just prior to the appearance of EADs.

at an action potential duration of 1200 ms ( $n=14$  myocytes). Following this, the action potentials began to rapidly repolarize.

A possibility is that the marked action potential prolongation at more positive voltages found with ATX II could cause an increase in intracellular  $\text{Na}^+$  and  $\text{Ca}^{2+}$ . In turn, this could lead to activation of  $\text{Ca}^{2+}$ -dependent currents which might cause the irregular low amplitude membrane voltage oscillations and EADs. To test for this, the sarcoplasmic reticulum modulator ryanodine ( $5 \mu\text{M}$ ) and the sarcoplasmic reticulum  $\text{Ca}^{2+}$  release inhibitor thapsigargin ( $1 \mu\text{M}$ ) were added to the bath of five cells with ATX II-induced EADs. Their addition rapidly abolished cell shortening, but did not antagonize the ATX II effects on the action potentials as shown in Figure 5. Similar findings were obtained in the four additional cells studied. In contrast, the  $\text{Na}^+$  channel blocker TTX ( $0.5 \mu\text{M}$ ) shortened action potential duration and suppressed the irregular low amplitude membrane voltage oscillations (Figure 6) with this finding confirmed in four cells.

## Discussion

This is the first report comparing the E-4031 and ATX II LQT models studied in single myocytes. The most significant finding of this work is that the E-4031 and ATX II models

produced strikingly different effects on action potential and EAD properties. The major differences are that ATX II, compared with E-4031, caused: (1) greater action potential prolongation; (2) more positive plateau voltages; (3) lower amplitude EADs with less negative take-off potentials; (4) greater time to the EAD peak voltage; and (5) longer duration EADs. Despite causing greater action potential prolongation, the frequency of EAD induction was much less with the ATX II model (28%) than with the E-4031 model (84%).

These experiments used a perforated patch clamp technique which is likely to be important in our findings. This patch clamp method avoids intracellular dialysis with pipette contents (such as  $\text{Ca}^{2+}$  buffers), and the diffusion of molecules and soluble proteins out of cells. In turn, this minimizes the rundown of several ion channel currents, drug sensitivity is increased, and changes in cell  $\text{Ca}^{2+}$  and cell contraction are maintained (see Zhou & January, 1998 for discussion). Since L-type  $\text{Ca}^{2+}$  channels are postulated to serve as the charge carrier for plateau EADs (January & Riddle, 1989; Zeng & Rudy, 1995), its preservation particularly important when studying EAD models. This may help to explain the infrequent reports of EAD properties studied using the conventional ruptured patch method.

E-4031 is a methanesulphonamide antiarrhythmic drug that selectively blocks  $\text{I}_{\text{Kr}}$  and the *human-ether-a-go-go-related*

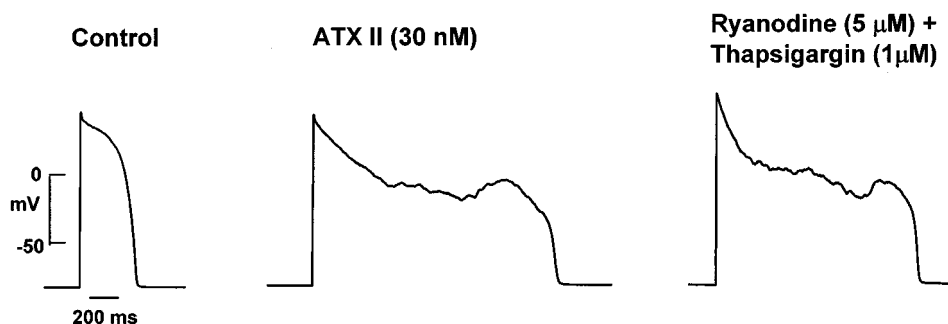


**Figure 5** Effect of ryanodine (5  $\mu\text{M}$ ) and thapsigargin (1  $\mu\text{M}$ ) on the action potential and an EAD. The left panel shows the control action potential. The middle panel shows action potential prolongation along with irregular low amplitude membrane voltage oscillations and an EAD after exposure to ATX II (30 nM). The right panel shows that ryanodine and thapsigargin did not suppress the ATX II-induced activity. Data from the same cell.

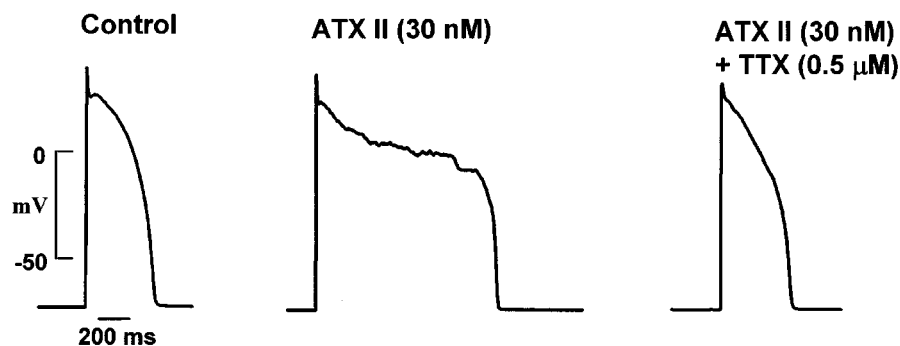


**Figure 6** Effect of TTX (0.5  $\mu\text{M}$ ) on the action potential. The left panel shows the control action potential. The middle panel shows ATX II-induced action potential prolongation accompanied by irregular low amplitude membrane voltage oscillations and an EAD. The addition of TTX shortened action potential duration and suppressed the irregular low amplitude membrane voltage oscillations as shown in the right panel. Data from the same cell.

gene (*HERG*) channel that encodes the pore-forming subunit (Sanguinetti & Jurkiewicz, 1990; Sanguinetti *et al.*, 1995; Trudeau *et al.*, 1995). The drug concentration used in these experiments reduced  $I_{K_r}$  tail current amplitude in rabbit ventricular cells by about 50% (Vorperian *et al.*, 1996). These channels generate their maximal repolarizing current at voltages near the action potential plateau (Zhou *et al.*, 1998), and their suppression with drugs such as E-4031 is a common mechanism for prolonging action potential duration and for initiating plateau EADs (Zhou *et al.*, 1994). In contrast, ATX II binds to the  $\text{Na}^+$  channel to slow inactivation from the open state resulting in prolonged channel bursting. This generates a maintained or slowly decaying inward  $\text{Na}^+$  current present over a broad range of voltages (Lazdunski *et al.*, 1980; Lawrence & Catterall, 1981; Warashina & Fujita, 1983; Isenberg & Ravens, 1984), which may account for ATX II induced action potential prolongation at more positive plateau voltages. The action potential prolongation by ATX II was uniformly accompanied by irregular low amplitude membrane voltage oscillations. This activity was previously reported to represent EADs (E1-Sherif *et al.*, 1990; Boutjdir *et al.*, 1994). Our findings using FFTs show that this activity lacked the frequency power spectrum pattern typical of plateau EADs. This activity also occurred at voltages positive to the recovery range of L-type  $\text{Ca}^{2+}$  window current (above 0 mV) needed for EAD depolarization (January & Riddle, 1989; Hirano *et al.*,

1992; Zeng & Rudy, 1995). The irregular low amplitude membrane voltage oscillations were not suppressed by ryanodine and thapsigargin, suggesting that  $\text{Ca}^{2+}$  overload and activation of  $\text{Ca}^{2+}$ -dependent currents was not essential. It was suppressed, however, by TTX which is consistent with a central role for  $\text{Na}^+$  channels. We conclude that the irregular low amplitude membrane voltage oscillations do not represent plateau EADs, rather they are likely to arise from current flowing with ATX II induced  $\text{Na}^+$  channel bursting during the action potential plateau. Our findings also provide evidence that the voltage of the action potential plateau, and not just its duration, is important in regulating EAD generation, and suggests that the QT interval on an ECG may not be the ideal measurement to define risks for arrhythmia provocation in LQT models.

#### *Clinical implications and limitations*

Extrapolation of our cellular electrophysiological data to the clinical syndrome is limited by incomplete understanding of LQT, in part due to the relatively small number of patients reported (particularly for LQT3), and because the phenotype of specific mutations within a gene defect may not be identical. None-the-less, our results may provide insight into previous clinical and experimental observations. In congenital LQT, the longest QT intervals usually are found in patients with LQT3 (Zareba *et al.*, 1998; Shimizu & Antzelevitch,

1999). These patients, however, have a lower frequency and cumulative probability of cardiac events when compared to patients with  $K^+$  channel mutations. Our findings provide a potential mechanism in that EADs occurred less frequently in the ATX II model, presumably because of the more positive plateau voltages that preceded repolarization. EADs are thought to be a critical cellular trigger for the initiation of torsades de pointes with the arrhythmia maintained by a re-entrant mechanism that depends on cellular and transmural differences in repolarization properties (El-Sherif *et al.*, 1996; 1997; Antzelevitch *et al.*, 1996). Although the cumulative probability of a cardiac event is lower in LQT3 patients, it also has been suggested that the risk of death during a cardiac event is higher in these patients (Zareba *et al.*, 1998). Our data show that EADs in the ATX II model occurred later in the action potential than those found with the E-4031 model. Because gradients of dispersion of repolarization are increased with increasing QT interval (Shimizu & Antzelevitch, 1999), the initiation of an EAD at a longer QT interval in LQT3 potentially could produce a more favourable substrate for a sustained arrhythmia and sudden death. Thus, differences in the cellular electrophysiological properties may account for differences in action potential prolongation and the induction of EADs, which may contribute to the clinical presentation of LQT.

## References

- ANTZELEVITCH, C., SUN, Z.Q., ZHANG, Z.Q. & YAN, G.X. (1996). Cellular and ionic mechanisms underlying erythromycin-induced long QT intervals and torsade de pointes. *J. Am. Coll. Cardiol.*, **28**, 1836–1848.
- BERGLAND, G.D. (1969). A guided tour of the fast Fourier transform. *IEEE Spectrum*, **2**, 41–52.
- BOUTJDIR, M. & EL-SHERIF, N. (1991). Pharmacological evaluation of early afterdepolarizations induced by sea anemone toxin (ATX II) in dog heart. *Cardiovasc. Res.*, **25**, 815–819.
- BOUTJDIR, M., RESTIVO, M., WEI, Y., STERGIPOULOS, K. & EL-SHERIF, N. (1994). Early afterdepolarization formation in cardiac myocytes: analysis of phase plane patterns, action potential, and membrane currents. *J. Cardiovasc. Electrophysiol.*, **5**, 609–620.
- BURASHNIKOV, A. & ANTZELEVITCH, C. (2000). Block of I(Ks) does not induce early afterdepolarization activity but promotes beta-adrenergic agonist-induced delayed afterdepolarization activity. *J. Cardiovasc. Electrophysiol.*, **11**, 458–465.
- CARMELIET, E. (1992). Voltage- and time-dependent block of the delayed  $K^+$  current in cardiac myocytes by dofetilide. *J. Pharmacol. Exp. Ther.*, **262**, 809–817.
- CLAY, J.R., OGBAGHEBRIEL, A., PASQUETTA, T., SASYNIUK, B.I. & SHRIER, A. (1995). A quantitative description of the E-4031-sensitive repolarization current in rabbit ventricular myocytes. *Biophys. J.*, **69**, 1830–1837.
- COLATSKY, T.J. & ARGENTIERI, T.M. (1994). Potassium channel blockers as antiarrhythmic drugs. *Drug Dev. Res.*, **33**, 235–249.
- D'ALONZO, A.J., ZHU, J.L. & DARBRENZIO, R.B. (1997). Effects of class III antiarrhythmic agents in an in vitro rabbit model of spontaneous torsades de pointes. *Eur. J. Pharmacol.*, **369**, 57–64.
- ECKHARDT, L., HAVERKAMP, W., BORGGREFE, M. & BREITHARDT, G. (1999). Experimental models of torsades de pointes. *Cardiovasc. Res.*, **39**, 178–193.
- EL-SHERIF, N., CAREF, E.B., YIN, H. & RESTIVO, M. (1996). The electrophysiological mechanism of ventricular arrhythmias in the long QT syndrome. Tridimensional mapping of activation and recovery patterns. *Circ Res.*, **79**, 474–492.
- EL-SHERIF, N., CHINUSHI, M., CAREF, E.B. & RESTIVO, M. (1997). Electrophysiological mechanism of the characteristic electrocardiographic morphology of torsade de pointes tachyarrhythmias in the long-QT syndrome: detailed analysis of ventricular tridimensional activation patterns. *Circulation*, **96**, 4392–4399.
- EL-SHERIF, N., CRAELIUS, W., BOUTJDIR, M. & GOUGH, B. (1990). Early afterdepolarizations and arrhythmogenesis. *J. Cardiovasc. Electrophysiol.*, **2**, 145–158.
- EL-SHERIF, N., ZEILER, R.H., CRAELIUS, W., GOUGH, W.B. & HENKIN, R. (1988). QTU prolongation and polymorphic ventricular tachyarrhythmias due to bradycardia-dependent early afterdepolarizations. Afterdepolarizations and ventricular arrhythmias. *Circ. Res.*, **63**, 286–305.
- HIRANO, Y., MOSCUCCI, A. & JANUARY, C.T. (1992). Direct measurement of L-type  $Ca^{2+}$  window current in heart cells. *Circ. Res.*, **70**, 445–455.
- ISENBERG, G. & RAVENS, U. (1984). The effects of the Anemone sulcata toxin (ATX II) on membrane currents of isolated mammalian myocytes. *J. Physiol.*, **357**, 127–149.
- JANUARY, C.T. & RIDDLE, J.M. (1989). Early afterdepolarizations: Mechanism of induction and block. A role for L-type  $Ca^{2+}$  current. *Circ. Res.*, **64**, 977–990.
- JANUARY, C.T. & ZHOU, Z. (1997). Early afterdepolarizations: Mechanisms and possible role in arrhythmias. In *Electrocardiology '96: From the Cell to the Body Surface*. ed. Liebman, J. pp. 231–240. Singapore: World Scientific Inc.
- LAWRENCE, J.C. & CATTERALL, W.A. (1981). Tetrodotoxin-insensitive sodium channels. Binding of polypeptide neurotoxins in primary cultures of rat muscle cells. *Biol. Chem. J.*, **256**, 6223–6229.
- LAZDUNSKI, M., BALERNA, M., BARHANIN, J., CHICHEPORTICHE, R., FOSSET, M., FRELIN, C., JACQUES, Y., LOMBET, A., POUYSSEUR, J., RENAUD, J.F., ROMÉY, G., SCHWEITZ, H. & VINCENT, J.P. (1980). Molecular aspects of the structure and mechanism of the voltage-dependent sodium channel. *Ann. NY Acad. Sci.*, **358**, 169–182.

We gratefully acknowledge and thank the late Stephen H. Nellis, Ph.D. for expert assistance with the FFT analysis. We also thank Timothy J. Kamp, M.D., Ph.D. for reviewing the manuscript. This work was supported in part by HL60723 and the Oscar Rennebohm Foundation. Dr Zhou is a recipient of an American Heart Association Scientist Development Grant.

- MOSS, A.J., ZAREBA, W., BENHORIN, J., LOCATI, E.H., HALL, W.J., ROBINSON, R.J., SCHWARTZ, P.J., TOWBIN, J.A., VINCENT, G.M. & LEHMANN, M.H. (1995). ECG T-wave patterns in genetically distinct forms of the hereditary long QT syndrome. *Circulation*, **92**, 2929–2934.
- RAE, J.L. & COOPER, K. (1990). New techniques for the study of lens electrophysiology. *Exp. Eye Res.*, **50**, 603–614.
- RODEN, D.M. (1993). Current status of class III antiarrhythmic drug therapy. *Am. J. Cardiol.*, **72**, 44B–49B.
- SANGUINETTI, M.C., JIANG, C., CURRAN, M.E. & KEATING, M.T. (1995). A mechanistic link between an inherited and an acquired cardiac arrhythmia: HERG encodes the  $I_{K_r}$  potassium channel. *Cell*, **81**, 299–307.
- SANGUINETTI, M.C. & JURKIEWICZ, N.K. (1990). Two components of cardiac delayed rectifier  $K^+$  current. Differential sensitivity to block by class III antiarrhythmic agents. *J. Gen. Physiol.*, **96**, 195–215.
- SHIMIZU, W. & ANTZELEVITCH, C. (2000). Differential effects of  $\beta$ -adrenergic agonists and antagonists in LQT1, LQT2 and LQT3 models of the long QT Syndrome. *J. Am. Coll. Cardiol.*, **35**, 778–786.
- SHIMIZU, W., MCMAHON, B. & ANTZELEVITCH, C. (1999). Sodium pentobarbital reduces transmural dispersion of repolarization and prevents torsades de pointes in models of acquired and congenital long QT syndrome. *J. Cardiovasc. Electrophysiol.*, **10**, 154–164.
- STUDENIK, C., ZHOU, Z. & JANUARY, C.T. (1996). Pharmacological models of long QT syndromes: Implications for drug therapy and ion channel defects (abstract). *Circulation*, **94**, I–642.
- STUDENIK, C., ZHOU, Z. & JANUARY, C.T. (1999). Differences in cellular electrophysiological and early afterdepolarization properties in two pharmacological models of LQTS (abstract). *Biophys. J.*, **76**, A366.
- TRUDEAU, M.C., WARMKE, J.W., GANETZKY, B. & ROBERTSON, G.A. (1995). HERG, a human inward rectifier in the voltage-gated potassium channel family. *Science*, **269**, 92–95.
- VORPERIAN, V.R., ZHOU, Z., MOHAMMAD, S., HOON, T.J., STUDENIK, C. & JANUARY, C.T. (1996). Torsades de pointes with an antihistamine metabolite: Potassium channel block with desmethylastemizole. *J. Am. Coll. Cardiol.*, **28**, 1556–1561.
- WARASHINA, A. & FUJITA, S. (1983). Effect of sea anemone toxins on the sodium inactivation process in crayfish axons. *J. Gen. Physiol.*, **81**, 305–323.
- ZABEL, M., HOHNLOSER, S.H., BEHRENS, S., LI, Y.G., WOOSLEY, R.L. & FRANZ, M.R. (1997). Electrophysiologic features of torsades de pointes: Insights from a new isolated rabbit heart model. *J. Cardiovasc. Electrophysiol.*, **8**, 1148–1158.
- ZAREBA, W., MOSS, A.J., SCHWARTZ, P.J., VINCENT, G.M., ROBINSON, J.L., PRIORI, S.G., BENHORIN, J., LOCATI, E.H., TOWBIN, J.A., KEATING, M.T., LEHMANN, M.H. & HALL, W.J. (1998). Influence of genotype on the clinical course of the long-QT syndrome. International Long-QT Syndrome Registry Research Group. *New Engl. J. Med.*, **339**, 960–965.
- ZENG, J. & RUDY, Y. (1995). Early afterdepolarizations in cardiac myocytes: mechanism and rate dependence. *Biophys. J.*, **68**, 949–964.
- ZHOU, Z., GONG, Q., YE, B., FAN, Z., MAKIELSKI, J.C., ROBERTSON, G.A. & JANUARY, C.T. (1998). Properties of HERG channels stably expressed in HEK 293 cells studied at physiological temperature. *Biophys. J.*, **74**, 230–241.
- ZHOU, Z. & JANUARY, C.T. (1998). Both T- and L-type  $Ca^{2+}$  channels can contribute to excitation-contraction coupling in cardiac Purkinje cells. *Biophys. J.*, **74**, 1830–1839.
- ZHOU, Z., STUDENIK, C. & JANUARY, C.T. (1994). Mechanisms of early afterdepolarizations induced by block of  $I_{K_r}$  (abstract). *Circulation*, **92**, I–435.
- ZHOU, Z., STUDENIK, C. & JANUARY, C.T. (1995). Properties of E-4031-induced early afterdepolarizations in rabbit ventricular myocytes: Studies using a perforated patch method. In *Potassium Channels in Normal and Pathological Conditions*. eds. Vereecke, J., van Bogaert, P.P. & Verdonck, F.P. pp. 375–379. Leuven: Leuven University Press.

(Received August 7, 2000  
Accepted October 12, 2000)